Fluorogenic Coumarins Activated via Bioorthogonal Reaction

Halley M. Lin-Jones, Sharon Chen, Yeonseong Seo, Kelly Q. Pham, Jennifer A. Prescher*

Department of Chemistry, University of California, Irvine, California 92697, United States

ABSTRACT: Fluorogenic bioorthogonal reagents enable facile detection in complex environments. While useful for real-time imaging, few such probes are available. Existing tools also exploit similar mechanisms for signal turn-on, precluding multiplexed applications. To address these gaps, we developed a palette of cyclopropenone (CpO) scaffolds that are activated by bioorthogonal phosphines to provide coumarins. The top CpO-phosphine pairs show strong fluorescent enhancements (up to 760-fold) and high quantum yields, and are stable in aqueous environments. The CpO fluorogens also exhibit unique reaction profiles, setting the stage for multi-component labeling studies.

Elucidating biomolecule functions in cellular environments is often dependent on imaging tools. One popular and general approach relies on ultra-selective bioorthogonal reactions to deliver detectable probes to targets of interest.[1,2] A unique functional group is first installed on the target, followed by selective labeling with a complementary reagent affixed to a fluorophore. The fluorescent label is typically provided in large excess to drive the reaction to completion, thus necessitating copious washing steps to remove unbound probe and reduce unwanted background signal. This limitation can present a significant barrier to imaging dynamic cellular processes.

To address the need for real-time imaging methods, fluorogenic bioorthogonal tools have been developed. These probes emit strong fluorescence upon ligation.[3,4] In contrast to "always-on" probes, the fluorogens can be supplied in excess to promote the reaction, without compromising the imaging readout. One widely used class comprises BODIPY-tetrazine conjugates. These reagents are quenched in the presence of the tetrazine, but fluorescence is restored upon reaction with strained alkenes.[5–7] Several related turn-on probes have been reported, but they are difficult to use in tandem. The tools rely on similar reaction mechanisms and can thus cross-react with one another.

To address the need for more versatile and mutually orthogonal imaging tools, we are leveraging a unique reaction between cyclopropenones (CpOs) and phosphines.[8–10] The reaction proceeds via conjugate addition of the phosphine to form a ketene-ylide intermediate; this electrophile is subject to trapping with a variety of nucleophiles. When the trapping moiety is part of the CpO itself, fluorescent adducts can result. We previously reported a CpO probe (**1**) of this sort. Upon phosphine treatment, a fluorescent coumarin adduct is formed (**Figure 1A**).[11] This transformation provides high signal-to-noise ratios and signal turn-on comparable to top fluorogenic tools. Cellular applications of the probe, though, remain limited. Strong UV excitation is required for detection. Additionally, the resulting coumarin fluorophore (**2**) exhibits a modest quantum yield.

Herein we report an expanded set of bioorthogonal CpO-masked coumarin probes with improved utility for biological imaging (**Figure 1B**). We exploited classic modifications known to enhance coumarin brightness, increase photostability, and alter emission profiles. The probes were screened with a variety of phosphines to identify suitable bioorthogonal turn-on triggers. Unique phosphine-CpO pairs were identified, setting the stage for multiplexed imaging.

One class of targeted scaffolds (naphCpOs **3** and **4**) comprised pi-extended naphthol cores. These designs were inspired by benzo[*g*]coumarins bearing electron-donating groups at the 7-position. Such probes generally display bright emissions and, in some cases, red-shifted wavelengths.[12,13] The second scaffold (julCpO **5**) featured the rigidified *N*-heterocycle, julolidine, found in many common dyes.[14–17] Julolidine modification has also been shown to red-shift the emission of some coumarins. The third target (azetCpO **6**) incorporated an azetidine at the 7-position in place of the original hydroxy group. This modification has been shown to dramatically enhance the photostability and thus photon output of common dyes.[17–19]

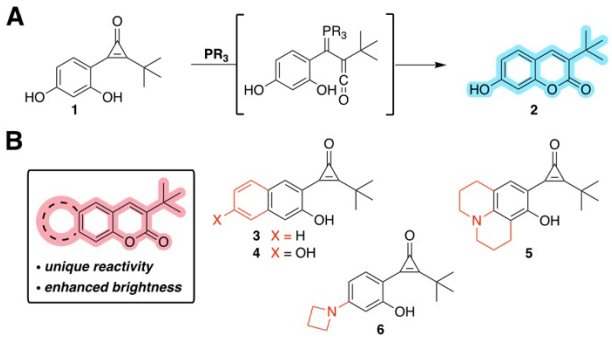

Figure 1. (A) Previously reported CpO **1** forms coumarin **2** via a ketene-ylide intermediate; (B) Functionalized CpO-masked coumarins **3**–**6** reported herein.

The targeted scaffolds were accessed from a common route, featuring a late-stage carbene insertion/hydrolysis sequence to deliver the requisite CpO functionality (**Scheme 1**). For naphCpO **3** the route began with commercially available 3-bromo-2-naphthol (**7a**), while naphthol precursor **7b** was prepared according to previously established methods.[20] The brominated starting materials were both acetyl-protected and subjected to Sonogashira coupling with *tert*-butylacetylene to afford **8a**–**b**. The critical dicarbene insertions followed[21], and upon silica-mediated oxidation, provided access to the key CpO moieties. Removal of the acetyl groups ultimately yielded the naphCpO probes **3** and **4**.

Scheme 1. Synthesis of (A) naphCpOs **3** and **4**, (B) julCpO **5**, (C) azetCpO **6**.

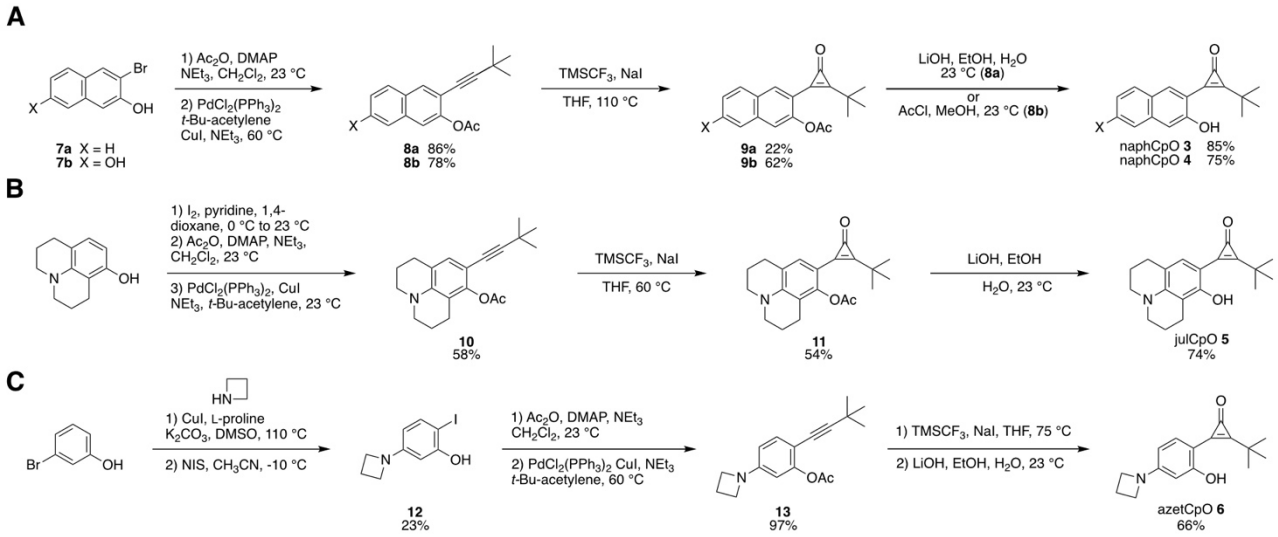

JulCpO **5** and azetCpO **6** were constructed similarly, with a few exceptions. To prepare julCpO **5**, we initially brominated commercially available 8-hydroxyjulolidine using *N*-bromosuccinimide, and then protected the phenol. However, subsequent Sonogashira coupling attempts were unsuccessful. We then prepared the more reactive aryl iodide using pyridine-mediated iodination, which facilitated formation of the desired alkyne in the Sonogashira coupling. Significant degradation of the aryl iodide was observed during purification, though, so the acetylation and coupling steps were completed sequentially without isolating the intermediate. The more stable alkyne **10** was ultimately subjected to the difluorocarbene and hydrolysis sequence to install the key CpO group.

Preparation of azetCpO **6** commenced with installation of the azetidine using Cu-catalyzed coupling conditions[22]. Similar methods have been used to install pyrrolidines and larger N-heterocyclic rings onto coumarin precursors.[23] The resulting intermediate was then treated with *N*-iodosuccinimide at reduced temperatures to yield aryl iodide **12**. This compound was notably more stable than the corresponding intermediate in the julCpO route. Aryl iodide **12** was further subjected to the acetylation and Sonogashira coupling sequence, followed by the final carbene insertion and hydrolysis steps to produce azetCpO **6**.

With the CpO fluorogens in hand, we aimed to test them with various phosphines to assess fluorescence turn-on. Phosphine addition can occur at either of vinyl units of the CpO moiety; only in one case would a fluorogen result (**Figure 2A**). Controlling the regioselectivity is key to developing robust tools, but often difficult to modulate with steric modifications alone.[11] The site of addition can also vary depending on the phosphine.

To more quickly identify suitable phosphine triggers for follow-up analyses, we used an initial fluorescence screen. Fluorescence emission would thus track with CpO-phosphine pairs capable of forming coumarin products in high yield. Toward this end, solutions of CpO probes **3**–**6** were prepared (10 mM in 4:1 CH_3CN:H_2O) and treated with commercially available phosphines. The panel included reagents with varying nucleophilicities, steric encumbrance, and polar appendages (**Figure 2A**). Excess phosphine (100 mM) was used to drive the reaction in all cases. After 24 hours, samples were visually inspected under a handheld UV-lamp to assess signal turn-on. Spectroscopic measurements were taken, and robust fluorescence was observed for various combinations.

AzetCpO **6**, in particular, formed a strongly emissive product with both triphenylphosphine (TPP) and cyclohexyldiphenylphosphine (CyDPP, **Figure 2B**). A similar trend was observed for julCpO **5**. Both CpOs **5** and **6** exhibited minimal fluorescence with the more nucleophilic alkyl phosphines, tris(hydroxypropyl) phosphine (THPP) and tris(2-carboxyethyl) phosphine (TCEP, **Figure 2C**). These results are consistent with our previous work demonstrating that added steric bulk around CyDPP, compared to THPP and TCEP, was essential for regioselective C2 addition in CpO **1**. However, the reduced emission observed with CpOs **5** and **6** could also be due to the 10-fold excess phosphine used in the screen itself, as phosphines are known to quench fluorophores under certain conditions.[24,25] No significant differences in light output were observed, though, when isolated azetidine coumarin **16a** was treated with up to a 10,000-fold excess of either TCEP or THPP (Figure S2). This result suggests that quenching by alkyl phosphines did not strongly bias the screening results. It was also possible that the emissions and reactions (especially with the alkyl phosphines) were impacted by the solvent. Screens in more aqueous solutions and at elevated pH values were difficult to conduct,

though, given the reduced solubilities of the reagents (Figure S1).

The phosphine screen revealed quite a different reactivity pattern for the naphthol CpOs. As shown in Figure 2C, naphCpOs **3** and **4** produced strong fluorescence only when treated with THPP. All other phosphines resulted in dim emission, suggesting that there was minimal conversion to the coumarin. This result was somewhat surprising and suggests that the expanded pi system of the probes impacts the regioselectivity of phosphine addition. We also observed that hydroxy-modified naphCpO **4** was 4-fold brighter than naphCpO **3**, demonstrating the importance of the electron-donating group on naphthalene core.

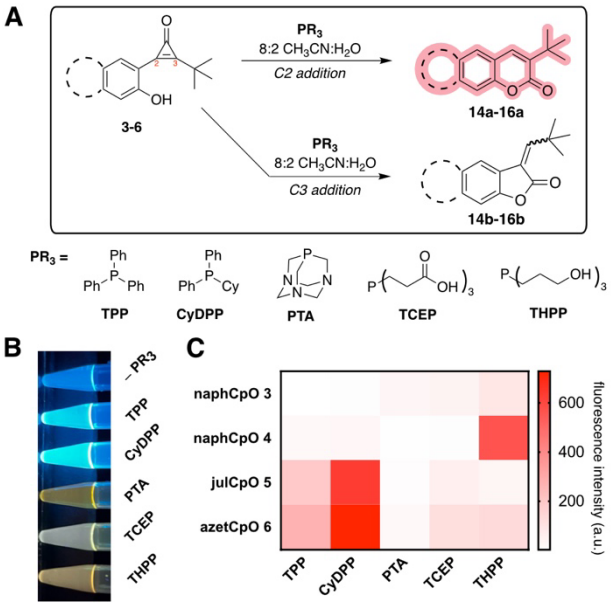

Figure 2. (A) CpOs **3**–**6** react with phosphines via C2 addition to form coumarins (**14a**–**16a**). C3 addition provides non-emissive furanone adducts (**14b**–**16b**); (B) Image of phosphine screen with azetidine-CpO **6**; (C) Heat map depicting maximum fluorescence emission intensity for each CpO-phosphine pair.

With the lead CpO-phosphine pairs identified from the screen, we pursued detailed characterization and kinetics studies. Initially, we isolated the fluorescent coumarins and measured their spectroscopic properties. Coumarins from naphCpO **4** and azetCpO **6** (naphCou **14a** and azetCou **16a**, respectively) displayed similar blue emission profiles to the original resorcinol coumarin **2** (**Figure 3A** and **Table 1**). The julolidine coumarin **15a**, by contrast, displayed a 16-nm red-shift in emission. We speculate that this red-shift can be further enhanced with additional tuning of the push-pull system.

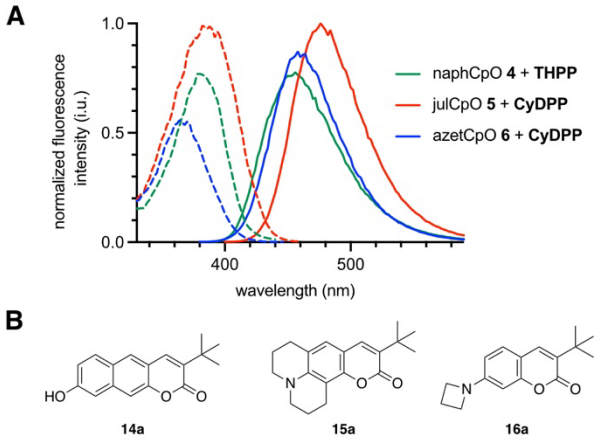

Figure 3. (A) Fluorescence excitation (dashed) and emission (solid) spectra for the brightest CpO-phosphine pairs: naphCpO **4** and THPP, julCpO **5** and CyDPP, and azetCpO **6** and CyDPP; (B) Structures of resulting coumarins **14a**, **15a**, and **16a** produced by the key CpO-phosphine reactions.

We also measured quantum yields to assess overall photon output, as well as the degree of fluorescence enhancement. The initial screen revealed that both julCpO **5** and azetCpO **6** reacted with CyDPP to produce brighter coumarins than those generated by the naphthol CpO **4** and THPP. As shown in **Table 1**, the quantum yields of julCpO **5** and azetCpO **6** and their resulting coumarins (**15a** and **16a**) were measured in 1:1 EtOH/PBS (pH 7.4). Gratifyingly, both julCou **15a** and azetCou **16a** displayed high quantum yields (**15a**, $\Phi = 0.88$; **16a**, $\Phi = 0.87$). The starting CpOs were minimally fluorescent, as predicted. Thus, the emission enhancements for CpO **5** and CpO **6** upon phosphine triggering are 300- and 760-fold, respectively. These probes are thus comparable to many of the brightest fluorogenic bioorthogonal probes in the field. It is worth noting, though, that the starting CpOs are strong absorbers (**5**, ε = 58,000; **6**, ε = 77,000). The amino and CpO substituents on the aryl ring constitute a good donor-acceptor pair. Further turning can likely modulate this parameter and decrease the relative brightness of the starting CpOs.

Table 1. Photophysical properties of fluorogenic CpOs and coumarin products.

Compound	λ_{abs} (nm)	λ_{exc} (nm)	λ_{em} (nm)	Φ	ε ($M^{-1}cm-1$)	Rel. brightness
julCou **15a**	394	382	476	0.88	35,000	740
julCpO **5**	357	384	474	0.0018	58,000	2.5
azetCou **16a**	360	361	463	0.87	37,000	760
azetCpO **6**	340	364	455	0.00054	77,000	1.0

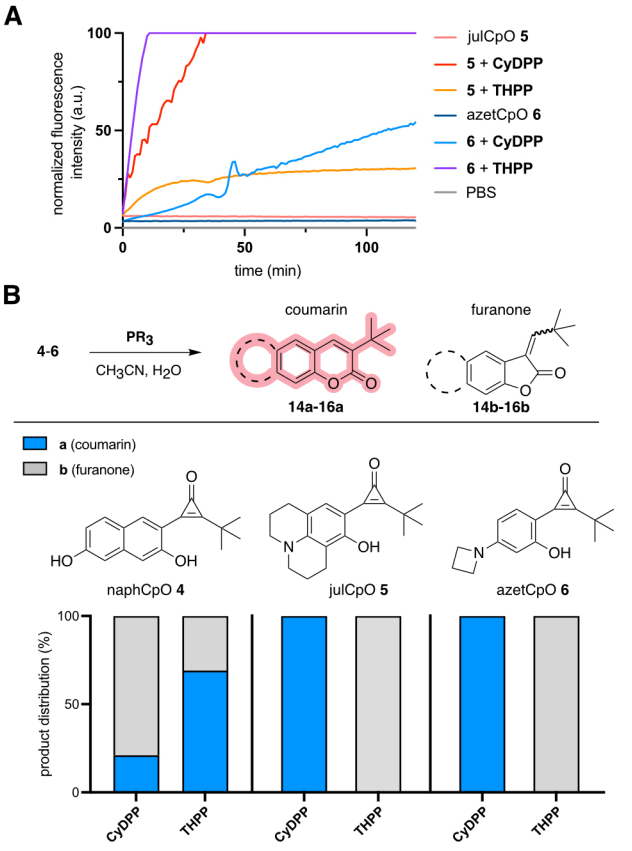

Figure 4. (A) Kinetic analysis of key CpO-phosphine reactions; (B) Product distributions observed for phosphine reactions with CpOs **4**–**6**.

Downstream biological applications of the CpO-phosphine pairs requires stable reagents with reasonable reaction rates. To assess the first parameter, we incubated CpOs **5** and **6** in aqueous solution, and monitored their longevity via ^{1}H-NMR spectroscopy. Both reagents were found to be stable over time. The probes were further subjected to L-cysteine, a biological nucleophile known to form covalent adducts with many electrophiles. The CpO fluorogens were also found to be stable under these conditions (Figure S3–S6).

Next, we studied the reaction kinetics for the key CpO-phosphine pairs. The rate of fluorophore formation was measured by preparing solutions of CpOs **5** and **6** (100 μM) in 10% DMSO and 90% PBS, then supplying the phosphine at varying concentrations (1–5 mM). The apparent second-order rate constants for the CpO-CyDPP reactions were determined to be 0.067 $M^{-1}s^{-1}$ and 0.0048 $M^{-1}s^{-1}$ for julCpO **5** and azetCpO **6**, respectively. We hypothesize that the electron-rich julolidine core enhances the reaction speed. While the transformations are slow compared to many gold-standard bioorthogonal transformations, the rate for julCpO **6** is comparable to those measured for previously reported resorcinol CpO **1**. Additionally, the fluorogenicity and enhanced brightness of these probes makes them detectable at remarkably low concentrations, mitigating the need for complete and rapid conversion.

Interestingly, azetCpO **6** reacted most rapidly with THPP with an apparent second-order rate constant of 0.016 $M^{-1}s^{-1}$. This reaction pair produced minimal fluorescence in the initial screen. We attribute the apparent discrepancy to the kinetics assay itself. Only the fluorescent adduct is detected, and while it is in low abundance, it is highly fluorescent. Analyses of the reaction samples by ^{1}H-NMR spectroscopy verified that the non-emissive furanone was the major product formed. The coumarin product was below the threshold of detection (<5%).

To further investigate the regioselectivity of the fluorogenic reactions, we quantified the ratio of coumarin and nonemissive furanone products for each CpO-phosphine pair (**Figure 4A**). The reactions were carried out in 4:1 CH_3CN:H_2O, and the products were isolated and characterized. As predicted, naphCpO **4** reacted with THPP to preferentially form the emissive coumarin **14a** (75% yield), whereas 25% of the isolated product was the furanone product **14b**. By contrast, naphCpO **4** reacted with CyDPP to form only 21% of coumarin **14a**. Excitingly, julCpO **5** and azetCpO **6** reacted with CyDPP to exclusively form the respective coumarin products. We envision that these unique reactivity profiles could be exploited for multiplexed imaging applications.

In summary, we developed a panel of fluorogenic CpO reagents with enhanced imaging properties. The most promising probes, julCpO **5** and azetCpO **6**, generate coumarins that are significantly brighter than the starting CpO structures. We additionally identified that naphthol-based CpOs exhibit a different reactivity profile than the other CpOs in this study, preferentially forming the coumarin structure when reacted with a more nucleophilic alkyl phosphine. Future directions will focus on applying the characterized probes to labeling biomolecules, as well as exploring the possibility of mutually orthogonal CpO probes.

ACKNOWLEDGMENT

This work was supported by the Chan Zuckerberg Initiative (2021-234603 to J.A.P.) We thank the UCI Mass Spectrometry Facility, the UCI NMR Facility, and the Laser Spectroscopy Labs for assistance with experiments. Additionally, we thank current and former members of the Prescher lab for helpful discussions.

REFERENCES

(1) Scinto, S. L.; Bilodeau, D. A.; Hincapie, R.; Lee, W.; Nguyen, S. S.; Xu, M.; Am Ende, C. W.; Finn, M. G.; Lang, K.; Lin, Q.; Pezacki, J. P.; Prescher, J. A.; Robillard, M. S.; Fox, J. M. Bioorthogonal Chemistry. *Nat. Rev. Methods Primer* **2021**, *1* (1), 30. https://doi.org/10.1038/s43586-021-00028-z.

(2) Sletten, E. M.; Bertozzi, C. R. Bioorthogonal Chemistry: Fishing for Selectivity in a Sea of Functionality. *Angew. Chem. Int. Ed.* **2009**, *48* (38), 6974–6998. https://doi.org/10.1002/anie.200900942.

(3) Shieh, P.; Bertozzi, C. R. Design Strategies for Bioorthogonal Smart Probes. *Org Biomol Chem* **2014**, *12* (46), 9307–9320. https://doi.org/10.1039/C4OB01632G.

(4) Chen, Y.; Jiang, H.; Hao, T.; Zhang, N.; Li, M.; Wang, X.; Wang, X.; Wei, W.; Zhao, J. Fluorogenic Reactions in Chemical Biology: Seeing Chemistry in Cells. *Chem. Biomed. Imaging* **2023**, *1* (7), 590–619. https://doi.org/10.1021/cbmi.3c00029.
(5) Carlson, J. C. T.; Meimetis, L. G.; Hilderbrand, S. A.; Weissleder, R. BODIPY–Tetrazine Derivatives as Superbright Bioorthogonal Turn-on Probes. *Angew. Chem. Int. Ed.* **2013**, *52* (27), 6917–6920. https://doi.org/10.1002/anie.201301100.
(6) Yang, J.; Šečkutė, J.; Cole, C. M.; Devaraj, N. K. Live-Cell Imaging of Cyclopropene Tags with Fluorogenic Tetrazine Cycloadditions. *Angew. Chem.* **2012**, *124* (30), 7594–7597. https://doi.org/10.1002/ange.201202122.
(7) Wu, H.; Yang, J.; Šečkutė, J.; Devaraj, N. K. In Situ Synthesis of Alkenyl Tetrazines for Highly Fluorogenic Bioorthogonal Live-Cell Imaging Probes. *Angew. Chem.* **2014**, *126* (23), 5915–5919. https://doi.org/10.1002/ange.201400135.
(8) Shih, H.-W.; Prescher, J. A. A Bioorthogonal Ligation of Cyclopropenones Mediated by Triarylphosphines. *J. Am. Chem. Soc.* **2015**, *137* (32), 10036–10039. https://doi.org/10.1021/jacs.5b06969.
(9) Row, R. D.; Shih, H.-W.; Alexander, A. T.; Mehl, R. A.; Prescher, J. A. Cyclopropenones for Metabolic Targeting and Sequential Bioorthogonal Labeling. *J. Am. Chem. Soc.* **2017**, *139* (21), 7370–7375. https://doi.org/10.1021/jacs.7b03010.
(10) Row, R. D.; Nguyen, S. S.; Ferreira, A. J.; Prescher, J. A. Chemically Triggered Crosslinking with Bioorthogonal Cyclopropenones. *Chem. Commun.* **2020**, *56* (74), 10883–10886. https://doi.org/10.1039/D0CC04600K.
(11) Heiss, T. K.; Dorn, R. S.; Ferreira, Andrew. J.; Love, A. C.; Prescher, J. A. Fluorogenic Cyclopropenones for Multicomponent, Real-Time Imaging. *J. Am. Chem. Soc.* **2022**, *144* (17), 7871–7880. https://doi.org/10.1021/jacs.2c02058.
(12) Jung, Y.; Jung, J.; Huh, Y.; Kim, D. Benzo[*g*]coumarin-Based Fluorescent Probes for Bioimaging Applications. *J. Anal. Methods Chem.* **2018**, *2018*, 1–11. https://doi.org/10.1155/2018/5249765.
(13) Kim, D.; Xuan, Q. P.; Moon, H.; Jun, Y. W.; Ahn, K. H. Synthesis of Benzocoumarins and Characterization of Their Photophysical Properties. *Asian J. Org. Chem.* **2014**, *3* (10), 1089–1096. https://doi.org/10.1002/ajoc.201402107.
(14) Kaur, P.; Singh, K. Julolidine-Based Probes for Detection of Analytes. *Dyes Pigments* **2023**, *220*, 111716. https://doi.org/10.1016/j.dyepig.2023.111716.
(15) Ismail, I.; Wang, D.; Wang, Z.; Wang, D.; Zhang, C.; Yi, L.; Xi, Z. A Julolidine-Fused Coumarin-NBD Dyad for Highly Selective and Sensitive Detection of H2S in Biological Samples. *Dyes Pigments* **2019**, *163*, 700–706. https://doi.org/10.1016/j.dyepig.2018.12.064.
(16) Jones, G.; Jackson, W. R.; Kanoktanaporn, S.; Halpern, A. M. Solvent Effects on Photophysical Parameters for Coumarin Laser Dyes. *Opt. Commun.* **1980**, *33* (3), 315–320. https://doi.org/10.1016/0030-4018(80)90252-7.
(17) Bassolino, G.; Nançoz, C.; Thiel, Z.; Bois, E.; Vauthey, E.; Rivera-Fuentes, P. Photolabile Coumarins with Improved Efficiency through Azetidinyl Substitution. *Chem. Sci.* **2018**, *9* (2), 387–391. https://doi.org/10.1039/C7SC03627B.
(18) Grimm, J. B.; English, B. P.; Chen, J.; Slaughter, J. P.; Zhang, Z.; Revyakin, A.; Patel, R.; Macklin, J. J.; Normanno, D.; Singer, R. H.; Lionnet, T.; Lavis, L. D. A General Method to Improve Fluorophores for Live-Cell and Single-Molecule Microscopy. *Nat. Methods* **2015**, *12* (3), 244–250. https://doi.org/10.1038/nmeth.3256.
(19) Zhou, J.; Lin, X.; Ji, X.; Xu, S.; Liu, C.; Dong, X.; Zhao, W. Azetidine-Containing Heterospirocycles Enhance the Performance of Fluorophores. *Org. Lett.* **2020**, *22* (11), 4413–4417. https://doi.org/10.1021/acs.orglett.0c01414.
(20) Ramaotsoa, G. V.; Strydom, I.; Panayides, J.-L.; Riley, D. Immobilized Tetrakis(Triphenylphosphine)Palladium(0) for Suzuki–Miyaura Coupling Reactions under Flow Conditions. *React. Chem. Eng.* **2019**, *4* (2), 372–382. https://doi.org/10.1039/C8RE00235E.
(21) García-Domínguez, A.; West, T. H.; Primozic, J. J.; Grant, K. M.; Johnston, C. P.; Cumming, G. G.; Leach, A. G.; Lloyd-Jones, G. C. Difluorocarbene Generation from TMSCF $_3$: Kinetics and Mechanism of NaI-Mediated and Si-Induced Anionic Chain Reactions. *J. Am. Chem. Soc.* **2020**, *142* (34), 14649–14663. https://doi.org/10.1021/jacs.0c06751.
(22) Zhang, H.; Ma, C.; Zheng, Z.; Sun, R.; Yu, X.; Zhao, J. Synthesis of 2-Arylbenzofuran-3-Carbaldehydes *via* an Organocatalytic [3+2] Annulation/Oxidative Aromatization Reaction. *Chem. Commun.* **2018**, *54* (39), 4935–4938. https://doi.org/10.1039/C8CC02474J.
(23) Bao, X.; Wang, G.; Tian, C.; Dong, X.; Xu, G.; Li, F.; Chen, D. Er(OTf)3-Catalyzed Synthesis of Fluorescent 7-Aminocoumarins. *Tetrahedron* **2022**, *123*, 132994. https://doi.org/10.1016/j.tet.2022.132994.
(24) Vaughan, J. C.; Dempsey, G. T.; Sun, E.; Zhuang, X. Phosphine Quenching of Cyanine Dyes as a Versatile Tool for Fluorescence Microscopy. *J. Am. Chem. Soc.* **2013**, *135* (4), 1197–1200. https://doi.org/10.1021/ja3105279.
(25) Lemieux, G. A.; De Graffenried, C. L.; Bertozzi, C. R. A Fluorogenic Dye Activated by the Staudinger Ligation. *J. Am. Chem. Soc.* **2003**, *125* (16), 4708–4709. https://doi.org/10.1021/ja029013y.